Interpretation of Spectroscopic Markers of H-Bonds

Steve Scheiner*
Department of Chemistry and Biochemistry
Utah State University
Logan UT 84322-0300

Abstract

Quantum calculations are used to examine whether a AH··D H-bond is unambiguously verified by a downfield shift of the bridging proton's NMR signal or a red (or blue) shift of the AH stretching frequency in the IR spectrum. It is found that such IR band shifts will occur even if the two groups experience weak or no attractive force, or if they are drawn in so close together that their interaction is heavily repulsive. The mere presence of a proton-acceptor molecule can affect the chemical shielding of a position occupied by a proton-donor by virtue of its electron density, even if there is no H-bond present. This density-induced shielding is heavily dependent on position around the proton-acceptor atom, and varies from one group to another. Evidence of a H-bond rests on the measurement of a proton deshielding in excess of what is caused purely by the presence of the proton acceptor species.

*email: steve.scheiner@usu.edu

keywords: NMR chemical shielding; stretching frequency shift; IR spectra

INTRODUCTION

As arguably the most prevalent noncovalent interaction, and with the greatest influence on molecular structure and activity, it would be difficult to overstate the importance of the H-bond (HB) [1-4]. In the biological realm alone, HBs are an essential component in the structure and function of the main classes of biomolecules such as proteins, nucleic acids, and carbohydrates. This situation has motivated an immense body of literature over the years inquiring into the nature of the HB that shows no sign of abating any time soon. From its original AH··D formulation as involving only highly electronegative atoms O, N, and F, and with the lone pairs of D serving as electron source, the scope of the HB has grown enormously [5] over the years. Much less electronegative atoms such as S and Cl are now recognized as participants in HBs, and electrons may be donated from π-bonds and even σ-bonds [6-11]. A good deal of current literature has dealt with the CH group as a HB donor [12-27]. Indeed, even metal atoms are acknowledged [28-32] to be involved in H-bonding, in the capacities of both electron donors and acceptors. There has even been wide recognition that the concept of the HB can be further broadened by the substitution of the bridging H by other atoms such as halogens, chalcogens, pnicogens, and even tetrels with little loss in binding strength [33-51].

The importance of the HB has motivated the search for tools by which to diagnose their presence, and to gauge their strength. The most widely used such experimental tools are spectroscopic in nature [52-54]. It has been observed that the formation of a AH··D HB commonly results in a red shift of the A-H stretching frequency, relative to the nonbonded situation. This shift is typically accompanied by a broadening and intensification of the vibrational band. A second diagnostic arises within the context of NMR spectroscopy where the formation of a HB shifts the signal of the bridging proton downfield, i.e. lesser chemical shielding. Both of these diagnostics contain quantitative information as well, since the degree of shift is usually closely related to the strength of the HB.

Nonetheless, despite their widespread usage, there is an implicit question associated with these spectroscopic markers. As AH and D approach one another they may or may not engage in a HB. Just their simple approach, without any mutual perturbation of their electron clouds, and thus no HB formation, could in principle cause changes to the spectra. In the case of large molecules such as proteins for example, it is not uncommon for two groups to be placed in close proximity due to the large number of structural factors, some rather remote, that ultimately result in a given three-dimensional structure. While this proximity may suggest an attractive interaction, particularly if the two groups are arranged in a AH··D geometry normally associated with a HB, it is no guarantee that there is truly a HB present, or of even an attractive force at all.

This situation takes on special significance when examining interactions whose identity as a HB is not obvious or is in question. Perhaps, the most obvious example would be the search for CH··O HBs in proteins. While the presence of such bonds is now well acknowledged [55-59] in the general sense, their typically weak nature can complicate the determination as to whether a specific interaction falls into this category, or is merely an inconsequential proximity with no energetic consequence [60-64].

The current communication attempts to use quantum chemical methods to distinguish between those situations where a HB is present and those where it is absent. In each case, the calculations provide the spectroscopic data that would emerge from each situation. The ultimate goal is the determination of what spectroscopic markers are truly representative of a HB, and which are the result of the mere proximity of the two relevant groups.

The work begins with a situation where an attractive HB is clearly present, i.e. the water dimer. By squeezing the two waters together, the attraction turns repulsive: how do the spectroscopic markers react to this reversal? The same analysis is applied to a weaker CH··O HB. Is there a HB present at all, and how do the markers behave as any attraction is eliminated, by either squeezing the groups together or by rotating them so as to eliminate any attraction that might otherwise exist. In other words, can these markers differentiate between an attractive and repulsive configuration?

In the particular case of NMR spectroscopy, the downfield shift of the bridging proton is taken as a fingerprint of the formation of a HB. But this shift arises from two separate factors. Quantum calculations over the years have amply documented the loss of electron density around this proton arising from the formation of a HB, as this density shifts toward the remainder of the proton-donor molecule. But the mere proximity of the proton-acceptor molecule's electron cloud will also affect the shielding around the proton, even were there no HB-induced polarization whatsoever. The determination of the existence of a HB must therefore be able to differentiate between these two effects. Calculations are applied here which evaluate these two effects separately, to serve as a guide in distinguishing the spectroscopic effects truly associated with HB formation.

COMPUTATIONAL METHODS

Calculations were carried out with the Gaussian-09 [65] suite of programs. Geometry optimizations were performed with the aug-cc-pVTZ basis set at the MP2 level. Minima were verified by the absence of imaginary frequencies. Interaction energies were evaluated as the difference between the energy of the complex and the sum of individual monomers in their optimized geometries. The NMR chemical shielding caused by a given molecule at various points in space surrounding it was evaluated by the placement of dummy atoms at these locations, with no nuclei, electrons, or basis set orbitals. Partitioning of the total

interaction energy was effected via the Symmetry-Adapted Perturbation Theory (SAPT) method using the MOLPRO [66] program.

RESULTS

H-Bond Contraction and Misorientation

In the case of the water dimer, it is well known that the formation of the HB induces a red shift of the OH stretching frequency in the proton donor, and a downfield shift in the NMR signal of the bridging proton. The first line of Table 1 confirms this expectation, and provides quantitative estimates of these quantities. Specifically, the interaction energy between the two water molecules in the fully optimized dimer is attractive, -5.2 kcal/mol. As a result of forming this dimer, the chemical shielding of the bridging proton is reduced by 2.96 ppm, and the asymmetric OH stretching frequency is shifted to the red by 105 cm^{-1}, both relative to their values in the optimized water monomer.

The ensuing rows of Table 1 document the consequences of squeezing the two waters together, where the deviation of R(H··O) from its optimum value is designated ΔR. As expected the interaction energy is quickly reduced and becomes repulsive as the R(H··O) intermolecular distance is contracted by more than 0.4 Å. The NMR shielding, however, shows no such reversal. Δσ becomes progressively more negative as the shielding on the bridging proton is continually reduced even though the interaction has become highly repulsive. The same is true of the OH stretch frequency which becomes progressively smaller, although Δν does take a turn up toward less negative values at the extreme compression of 0.8 Å.

Similar data is collected in Table 2 for the $H_3CH\cdots OH_2$ heterodimer. This complex is considerably less strongly bound than is the water dimer, by less than 1 kcal/mol, as reported in the first row of Table 2, and the chemical shielding of the CH proton is reduced by roughly 1/3 as much. Rather than the red shift of the OH stretching frequency in the water dimer, the CH stretch shifts to the blue. This reversal of the usual pattern in the case of CH··O HBs is not unexpected, based on numerous reports [21,67-72] in the literature for this and similar systems. More importantly, just as in the case of the water dimer, the trends in both Δσ and Δν become more pronounced as the CH_4 and OH_2 molecules are squeezed together, and the potential reverses from attractive to repulsive. It may thus be concluded that the IR and NMR markers of HB formation do not behave like the energetics, but rather intensify the normal trends even if the HB is squeezed well beyond its attractive minimum.

Any intermolecular interaction results contains elements of both attractive and repulsive forces. The latter corresponds to Pauli exchange terms, similar to steric repulsions. The former is a sum of electrostatic attraction, coupled with induction and dispersion forces. The equilibrium geometry is achieved when the attractive and repulsive forces balance one another. Squeezing two molecules closer than their equilibrium separation will typically enhance the attractive force, but the repulsion will increase by a larger amount,

thereby causing the total energy to rise. The sum of all three attractive terms are displayed in the last column of Tables 1 and 2 where it may be seen to grow rapidly as the two molecules more closely approach one another. (It is the even more rapid growth of the steric repulsions which prevents a collapse.) The changes in NMR chemical shielding $\Delta\sigma$ correlate quite well with this total attractive element with a correlation constant for linear fitting of 0.99. The IR shifts, on the other hand, do not correlate as well. One can thus draw the inference that although the NMR signal of H-bonding behaves differently than does the total interaction energy, it is closely related to the attractive portion of the total.

In addition to weakening the CH··O HB by contraction of the R(H··O) distance, one can also rotate the water molecule in such a way as to turn the O lone pairs away from the approaching CH. The water was rotated such that one of its OH bonds was directly opposite the CH, and the remainder of the geometry optimized. The ensuing R(H··O) distance was very close, within 0.015 Å, of that in the fully optimized structure, and the interaction energy was little affected. The NMR $\Delta\sigma$ was changed from -1.0 to -0.6 ppm by this reorientation, and the IR OH shift increased from 1.5 to 2.1 cm^{-1}. Enforcing a second restriction, such that the CH··OH configuration is entirely linear, reduces the interaction energy by only 0.2 kcal/mol. The NMR shift is changed by only 0.1 ppm, and $\Delta\nu$ is raised to 3.6 cm^{-1}. Thus these geometric perturbations produce only marginal changes in the patterns noted above.

One might anticipate that the substitution of the two H atoms by the much more electron-withdrawing F might make the O lone pairs less available for participation in a CH··O HB with CH_4, and thus weaken this bond. This expectation is unfulfilled however: CH_4 is bound to OF_2 by 0.79 kcal/mol. The formation of this CH··O HB reduces the chemical shielding of the bridging proton by 0.53 ppm, about half of that computed for $H_3CH··OH_2$, and the CH stretching shift is +3.6 cm^{-1}, nearly four times larger.

In summary, the NMR and IR spectroscopic markers are unable to distinguish between an attractive HB interaction, and the repulsion resulting from radial and angular distortions of the preferred geometry.

Carbonyl and Hydroxyl Groups

The carbonyl group is interesting in that a CH proton donor can approach from a number of different directions. Approach toward the O atom is expected to lead to an attractive CH··O HB. The structure exhibited in Fig 1a is indeed bound by 0.79 kcal/mol. The bridging proton's chemical shielding is reduced by 1.46 ppm relative to the monomer, and the CH stretching frequency raised by 5.0 cm^{-1}. Approach of the CH toward the C atom of H_2CO from above the molecular plane is anticipated to be less attractive, and in fact the configuration shown in Fig 1b is bound by only 0.40 kcal/mol. The CH stretching frequency is raised but by only 3.0 cm^{-1}. Perhaps more interesting, the shielding of the bridging proton is not reduced as is the norm in HBs, but is instead increased, albeit by only 0.10 ppm.

Some insight into this behavior may be gained by examining the changes induced in the total electron density of each monomer by their approach toward one another, and the formation of any noncovalent bonds. The green regions in Fig 1c and 1d indicate increases of density, while losses are represented by yellow. Of particular note is the extensive yellow loss region surrounding the bridging proton in Fig 1c, consistent with its deshielding. This pattern may be compared with that of the CH··C configuration in Fig 1d, where the bridging proton lies within a green area of density gain, which would account for the increase in σ. But it must be noted as well that a yellow area of diminished density also lies quite close to the same proton, exerting an opposite effect.

One of the major factors that affects the shielding around the bridging proton is of course the electron redistribution patterns in Fig 1, which result from the interaction between the two molecules. But even in the absence of any interaction at all, and zero electron redistribution, the mere approach of the proton toward the second molecule would have some effect on its shielding, by virtue of the collection of nuclei and surrounding electron density. As an example, the shielding produced by the H_2CO molecule in Fig 1a, in the absence of CH_4, at the precise location of the bridging proton, 2.589 Å from the O atom, is -0.63 ppm. That is, of the total -1.46 ppm shielding change experienced by the proton of CH_4 in the full dimer, -0.63 can be attributed to the simple presence of the H_2CO, and the remaining -0.83 ppm to the electron density redistribution at this position caused by the field emanating from the H_2CO. Using the same protocol for the CH··C interaction in Fig 1b, the unperturbed H_2CO leads to an increase in the shielding by 0.26 ppm at the position of the methane H atom. The observation that the shielding change of the bridging proton within the context of the entire dimer is less positive, only 0.10 ppm, translates to a deshielding, by -0.16 ppm, of the proton attributed to the density redistribution caused by the interaction of the two molecules, i.e. the H-bond.

The chemical shielding caused solely by the electron cloud of the H_2CO molecule can be mapped out more systematically. Fig 2 shows the definition of θ as the deviation from the C=O direction within the plane of the molecule, and φ the tilt out of the molecular plane. The shielding was computed as a function of both θ and φ for four separate distances R from the carbonyl O center. The dependence upon the in-plane θ angle is illustrated in Fig 2a, where one can see that the shielding is most negative directly along the C=O axis. That is, the field of the H_2CO molecule in that direction would tend to deshield any entity placed here. It becomes progressively less negative as the point is moved around toward the “rabbit ear” lone pairs at roughly 60°, after which there is a tendency toward more deshielding. The trends are the same for all distances, but are more intense for shorter values of R. Like the in-plane deformations, the out-of-plane distortions in Fig 2b also become less negative as the point moves away from the C=O axis. The deshielding crosses the horizontal axis at about 35°, above which a shielding pattern is observed. This

deshielding is consistent with the pattern noted above for placement of the proton directly above the C atom. These data suggest that when a proton donor molecule is paired with a carbonyl acceptor, the mere finding of a deshielding of the proton would not be sufficient to establish the presence of a HB. The conclusion of a HB would require a deshielding more negative than the values in Fig 2, consistent with the polarization effects associated with HB formation.

It is interesting to compare the carbonyl O with its hydroxyl congener, which replaces the double C=O bond by a pair of single O-H bonds. The analogous data is presented in Fig 3 for the water molecule. Note that in-plane angle θ refers to the plane of the O lone pairs in each case, not to the molecular plane; values of 0° are referred to the HOH bisector for water. The shielding produced by the hydroxyl group is considerably smaller than that of the carbonyl group. With the exception of the very close R(H··O) distance of 1.5 Å, the shielding produced by HOH remains below 0.5 ppm, roughly 1/3 the extrema for H_2CO. Secondly, the shielding is less sensitive to misalignment with the HOH bisector, rising only gradually. Finally, there is little distinction between the in and out-of-plane behavior for the hydroxyl group. Perhaps most important, the shielding is usually positive, barely negative even at its minima, and never surpassing -0.02. In stark contrast to a carbonyl O, in the case of a hydroxyl group the measurement of even a fairly small deshielding can be taken as indicative of a HB.

Within the context of a protein, the most common proton acceptor atom is the carbonyl O of the backbone peptide group. Its presence as part of a peptide alters several of the characteristic behaviors of the carbonyl O atom, partly due to its participation in a sort of resonance with the C-N bond. The manner in which the peptide O differs from the simple carbonyl can be inferred from a comparison of Fig 2 with Fig 4, which characterizes N-methylacetamide (NMA) as a model of the peptide group.

Focusing first upon the chemical shielding within the plane of the peptide, it must first be noted that there is an asymmetry in that a positive value of θ refers to displacement toward the N atom, and motion away is designated by -θ. Nonetheless, the effects on the chemical shielding are mostly symmetrical, as evident in the upper panel of Fig 4. The exception occurs for large positive θ where the point of interest closely approaches the methyl group attached to the N atom. Deshielding occurs along the C=O axis with small values of θ, albeit only by a small amount with the absolute value of σ less than 0.5. These small values contrast sharply with the larger magnitude for the simple carbonyl of H_2CO in Fig 2. With the exception of R=1.5 Å, σ is nearly independent of θ, changing very little except when θ get large enough to interact with the methyl group. The flatness of these curves contrasts with the stronger sensitivity to θ of H_2CO. Whereas the in-plane behavior of NMA and H_2CO differ, there are strong similarities when the point is brought out of the plane, as is evident in a comparison of the lower panels of Figs 2 and 4. In both cases, σ becomes steadily more positive as φ grows, even if the absolute values are somewhat smaller for

NMA. Summarizing, in the areas where one might expect a proton donor to engage with the peptide carbonyl O, the deshielding which is a consequence of the mere presence of the NMA is on the order of -0.3 to -0.5 ppm. The establishment of a HB would thus mandate the measurement of proton deshielding that exceeds this range.

Carboxylate

In addition to its widespread occurrence in proteins as the sidechain of Asp and Glu, the carboxylate group also represents a variation on the carbonyl O theme. There are a pair of O atoms attached to the same C, and the entire group carries an overall negative charge. The manner in which the electron density of this group sets up chemical shielding in its vicinity is illustrated in Fig 5. Positive values of θ represent deviations away from the C-O axis toward the other O atom, while motions in the opposite direction are designated by negative values of θ. For each of a set of fixed angles, the curves in Fig 5 illustrate how the chemical shielding is affected as the observation point is pulled away to a distance R from the O atom.

In all cases, σ is very positive for small values of R, but diminishes quickly as the observation point moves away from the O. Taking the black θ=0° curve as an example, σ= 0.5 ppm when R=1.6 Å, then diminishes to 0 at 2.3 Å. Beyond that point, σ is slightly negative, with a maximal value of -0.018 ppm at R=2.8 Å. For the larger values of θ=30° and 60°, σ is more positive for small distances, and slightly more negative for longer R. At the largest angle 90°, one sees the most negative σ, reaching a minimum of -0.216 ppm at R=2.4 Å. When the reference point is moved in the opposite direction, toward negative θ, there is also a tendency toward more negative σ. In summary, only small negative values of σ are observed along the C-O axis, but angular deviations in either direction enhance these quantities to as much as -0.22 ppm. Deshielding of the putative H-bonding proton in excess of these quantities would be necessary to indicate the presence of a HB.

Imidazole

The imidazole (Im) sidechain of His engages in H-bonding quite commonly in proteins. It is only the neutral Im that will participate as proton acceptor, and that most often at the N atom that is not bonded to a H atom. The chemical shielding in the vicinity of the N atom of Im is displayed in Fig 6. The bisector of the C-N-C grouping, essentially the direction of the N lone pair, is taken as θ=0. The shielding that occurs both in and out of the Im plane may be seen in Fig 6 to be quite positive for small values of R, and then to rapidly diminish to negative quantities, before tapering off at long distance. Along the lone pair direction, σ reaches a minimum of -0.47 ppm at R=2.2 Å. This minimal value is enhanced for angular deviations, amounting to -0.71 ppm at R=2.0 Å when θ=30°. In contrast to in-plane displacements, the motion of the reference point out of the plane leads to progressively less negative σ. When φ=30°, the minimum occurs for σ= -0.23 ppm at R=2.4 Å. It is important to note that whether in or out of the molecular plane, σ is

consistently negative for all values of R beyond about 2 Å. One would thus expect even more negative deshielding of any putative H-bonding proton.

Aromatic Ring

In addition to classic H-bonds involving lone pairs as electron donor, there is a marked propensity for proton donors to situate themselves above an aromatic ring, in what is commonly referred to as a π H-bond. Such an arrangement is electrostatically favored since a phenyl ring contains a region of negative electrostatic potential above its plane, which could attract a proton donor. The π-electron system above the ring could in principle serve as electron donor. Even so, it is not obvious that arrangements of this sort constitute a true H-bond, or are instead the consequence of a simple Coulombic attraction, or even no more than a result of geometric constraints of the protein which push the two groups into coincidence with little or no attractive force. NMR analysis can in principle help answer this question, as a diagnostic for the presence of a H-bond. However, one must first understand how the fields generated by the phenyl ring might shield an approaching proton, even in the absence of any interaction, attractive or repulsive.

The shielding above the plane of a benzene molecule, as a model of the Phe aromatic ring, is illustrated in Fig 7. Each curve represents the shielding produced by the benzene electron density for a given distance R above the benzene plane. The displacement of the reference point from the center of the ring is represented by d, as indicated in Fig 7. Each curve in the figure is labeled with this displacement. Considering first the set of points directly above the benzene center, with d=0, the black curve in Fig 7 shows a high level of shielding, 10 ppm, for a point 1.0 Å above this central point. This shielding diminishes smoothly as the reference point is pulled further away but stays fairly large, even for R=4 Å. A small displacement of 0.2 Å (red curve) does not alter this result by much. As the displacement continues, one can see that σ becomes larger for small R, but decreases more dramatically as R is stretched. But in summary, all of the curves have a similar shape regardless of the displacement, even as much as d=1.3 Å. This latter displacement locates the point of reference almost directly above one of the benzene C atoms.

Given the universally positive values of σ above the ring plane, the polarization within a proton donor molecule that tends to deshield a proton might not be sufficient to overcome the shielding of the aromatic ring in Fig 7. Hence an overall increased shielding measured for this proton would not disprove the existence of a HB. Rather a shielding increase of lesser magnitude than in the figure might be taken as evidence that such a HB is indeed present.

DISCUSSION

The most well known and widely used spectroscopic markers of the presence of a AH··D H-bond are the shifts in the NMR chemical shielding of the bridging proton and the vibrational frequency of the A-H stretching mode. While these indicators undoubtedly occur in the presence of a H-bond, there is some

question as to whether the converse is true: can these same shifts also occur in the absence of a H-bond. The calculations indicate that the latter is correct, so that the observation of these shifts does not necessarily prove the existence of a H-bond. Instead, the measured data must be carefully compared with values anticipated were there no HB present.

In the case of the paradigmatic water dimer, the bridging proton suffers a loss of chemical shielding and the O-H stretching frequency redshifts upon formation of the HB. However, these same phenomena occur, and are in fact amplified, when the two molecules are squeezed together such that the intermolecular potential has become repulsive. Likewise for the weaker CH··O HB between CH_4 and OH_2. The C-H stretching frequency shifts to the blue in the optimized geometry, and this shift becomes even stronger in the repulsive region of the potential. These same shifts are observed also even when the CH_4 and OH_2 molecules are reoriented to eliminate any vestige of a HB.

Just the presence of a second molecule can affect the chemical shielding of a proton donor, even if the polarizing influence of a H-bond interaction is switched off. The nuclei and electron density of the acceptor molecule generate fields that are highly anisotropic, and can either shield or deshield a given point in its surroundings from an external magnetic field. Taking the carbonyl group of H_2CO as an example of an important proton acceptor, the calculations show that it will deshield along the C=O axis, and this deshielding diminishes as one moves toward the O lone pairs. Displacement out of the molecular plane reverses this deshielding into a shielding pattern.

The polarization of the AH bond that accompanies HB formation reduces the electron density around the bridging proton, and is thus responsible for a certain degree of deshielding. If such a AH··D HB is present, one would thus expect the observed deshielding to be larger than that due solely to the fields generated by the proton acceptor molecule. So for example, if the acceptor field is calculated to deshield a reference point by 1 ppm, then a true HB would result in a deshielding by a larger amount. Conversely, if the acceptor field has a shielding effect, as would occur above the carbonyl plane, then even a small amount of deshielding, or in fact no shielding at all, would be indicative of a HB.

The transition from a carbonyl to a hydroxyl oxygen produces significant changes in the shielding, so that the data for one are not translatable to the other. The hydroxyl group produces a generally smaller degree of shielding, less sensitive to the position of the reference point in the plane of the lone pairs, and with little difference between misalignments in or out of the lone pair plane. The enlargement of the carbonyl to an amide/peptide group also leads to important changes. The shielding within the molecular plane is rather insensitive to the direction, and amounts to a rather weak deshielding, less than -0.5 ppm. An observed larger degree of deshielding could thus be taken as evidence of a HB.

The carboxylate anion produces an overall deshielding effect in its vicinity, but this effect is rather small, not exceeding -0.2 ppm. One could thus safely deduce the presence of a true HB if the deshielding on the proton were of larger magnitude. The deshielding tapers off as the distance from the O atom is lengthened. A particularly short contact, less than about 2 Å produces a shielding. Somewhat greater deshielding, approaching -1 ppm, is associated with the unprotonated N atom of imidazole. This deshielding is maximized at a distance of roughly 2 Å, and is greatest for 30° deviations from the N lone pair direction. Because of the π-electron ring currents within an aromatic ring, positions above the plane are shielded, and by quite a large amount. For distances in the 2-3 Å range, for example, the shielding lies in the +2 to +5 ppm range. One could thus easily miss a π-HB if one were looking for a deshielding of the bridging proton. Even the downshift caused by a substantial H-bond induced polarization of the AH bond might not be able to counteract the shielding caused by the phenyl ring currents.

The ability of a molecule to respond to an external magnetic field, and to thus influence the chemical shielding of any nuclei in its vicinity is a well recognized phenomenon. A commonly accepted example of this sort of behavior arises in the context of π H-bonds where a proton donor approaches an aromatic system from directly above the ring. Aromatic ring current effects tend to shield any object in this position, which accounts for the upfield shifts observed for these sorts of HBs [73-76], effectively countering the deshielding effects engendered by the H-bond process itself. Indeed, a number of studies in the recent literature detail how the amount of this shielding is closely aligned with the degree of aromaticity or even antiaromaticity [77-81]. This sort of reasoning is not limited to aromatic systems. A recent work [82] extended the idea to small hydrocarbons such as butadiene, although it was concerned chiefly with shielding within the confines of each molecule itself, rather than its neighborhood. An earlier work is perhaps most pertinent in that [83] the shielding in the area surrounding molecules was explicitly examined. While limited to small hydrocarbons such as ethane and ethylene rather than HB acceptors, the results reinforce our own findings that the chemical shielding caused by a given system can be highly anisotropic.

The changes in the A-H stretching frequencies induced in the proton donor molecule by HB formation have an entirely different source. A number of different rationales have been proposed [14,72,84-94], but all frameworks are organized around a set of competing forces, some pulling the mode to lower frequency and others in the reverse direction. In the majority of HBs, the former forces are stronger, but blue shifts can occur when the latter overwhelm the former, with CH··O HBs the most common example. One can focus on recent experimental measurements [95] which attribute the direction of shift to the electric field generated by the proton acceptor molecule. Prior calculations [84,96-98] have shown how this field is directly related to stretches and/or contractions of the C-H bond, and thus to red/blue shifts of the vibrational frequency. One would not expect the field of the proton acceptor molecule to lessen if the proton donor approaches closer

than the equilibrium distance, even if the intermolecular potential has become repulsive. This notion is consistent with the finding that the A-H stretching frequency shifts of the water dimer and $H_3CH\cdot\cdot OH_2$ discussed above, either red or blue, become even more dramatic as the two molecules are compressed together. Nor will the field emanating from this molecule necessarily change in a drastic manner if the polarization and other phenomena attributed to a HB are absent. There is thus no reason to anticipate that frequency shifts are necessarily due exclusively to the presence of a HB. Other means of rationalizing the frequency shift eschew the electric field and focus instead on energy components such as exchange, electrostatics, polarization, etc. These components too would tend to simply enlarge as the two subunits are brought close enough together so that they are beyond the attractive part of the intermolecular potential.

In summary, the shift of the AH stretching frequency, red or blue, and the downfield shift of the bridging proton's NMR signal, are necessary but not sufficient demonstration of the presence of a H-bond. There is a certain amount of chemical shift that occurs purely by virtue of the proximity of the electron cloud of the second molecule; a H-bond's presence would be signaled by a shift in excess of this amount.

REFERENCES

[1] G. Gilli, P. Gilli. The Nature of the Hydrogen Bond; Oxford University Press: Oxford, UK, 2009.
[2] S. J. Grabowski, Ed. Hydrogen Bonding - New Insights; Springer: Dordrecht, Netherlands, 2006.
[3] G. A. Jeffrey, W. Saenger. Hydrogen Bonding in Biological Structures; Springer-Verlag: Berlin, 1991.
[4] S. Scheiner. Hydrogen Bonding: A Theoretical Perspective; Oxford University Press: New York, 1997.
[5] E. Arunan, G. R. Desiraju, R. A. Klein, J. Sadlej, S. Scheiner, I. Alkorta, D. C. Clary, R. H. Crabtree, J. J. Dannenberg, P. Hobza, H. G. Kjaergaard, A. C. Legon, B. Mennucci, D. J. Nesbitt, *Pure Appl. Chem.* **2011**, *83*, 1637-1641.
[6] H. S. Biswal. In Noncovalent Forces; Scheiner, S., Ed.; Springer: Dordrecht, Netherlands, 2015, p 15-45.
[7] H. S. Biswal, E. Gloaguen, Y. Loquais, B. Tardivel, M. Mons, *J. Phys. Chem. Lett.* **2012**, *3*, 755-759.
[8] M. Solimannejad, S. Scheiner, *Int. J. Quantum Chem.* **2011**, *111*, 3196-3200.
[9] G. Chalasinski, S. M. Cybulski, M. M. Szczesniak, S. Scheiner, *J. Chem. Phys.* **1989**, *91*, 7048-7056.
[10] Z. Latajka, S. Scheiner, *J. Chem. Phys.* **1987**, *87*, 5928-5936.
[11] S. J. Grabowski, *J. Phys. Org. Chem.* **2013**, *26*, 452-459.
[12] J. E. Del Bene, I. Alkorta, J. Elguero, *Phys. Chem. Chem. Phys.* **2011**, *13*, 13951-13961.
[13] S. Scheiner, *Curr. Org. Chem.* **2010**, *14*, 106-128.
[14] S. J. Grabowski, *J. Phys. Chem. A* **2011**, *115*, 12789-12799.
[15] S. A. C. McDowell, A. D. Buckingham, *Phys. Chem. Chem. Phys.* **2011**, *13*, 14097-14100.
[16] M. M. Szczesniak, G. Chalasinski, S. M. Cybulski, S. Scheiner, *J. Chem. Phys.* **1990**, *93*, 4243-4253.
[17] H. S. Biswal, S. Wategaonkar, *J. Phys. Chem. A* **2009**, *113*, 12774-12782.
[18] O. Takahashi, Y. Kohno, S. Iwasaki, K. Saito, M. Iwaoka, S. Tomoda, Y. Umezawa, S. Tsuboyama, M. Nishio, *Bull. Chem. Soc. Jpn.* **2001**, *74*, 2421-2430.
[19] S. Cybulski, S. Scheiner, *J. Am. Chem. Soc.* **1987**, *109*, 4199-4206.
[20] D. Mani, E. Arunan, *J. Chem. Phys.* **2014**, *141*, 164311.
[21] Y. Gu, T. Kar, S. Scheiner, *J. Mol. Struct.* **2000**, *552*, 17-31.
[22] N. Lu, R. M. Ley, C. E. Cotton, W.-C. Chung, J. S. Francisco, E.-I. Negishi, *J. Phys. Chem. A* **2013**, *117*, 8256-8262.
[23] B. Michielsen, C. Verlackt, B. J. van der Veken, W. A. Herrebout, *J. Mol. Struct.* **2012**, *1023*, 90-95.
[24] G. Sánchez-Sanz, C. Trujillo, I. Alkorta, J. Elguero, *Phys. Chem. Chem. Phys.* **2012**, *14*, 9880-9889.
[25] Z. Latajka, S. Scheiner, *J. Comput. Chem.* **1987**, *5*, 674-682.
[26] W. Zierkiewicz, D. Michalska, T. Zeegers-Huyskens, *Phys. Chem. Chem. Phys.* **2010**, *12*, 13681-13691.
[27] E. Kryachko, S. Scheiner, *J. Phys. Chem. A* **2004**, *108*, 2527-2535.
[28] F. Groenewald, J. Dillen, H. G. Raubenheimer, C. Esterhuysen, *Angew. Chem. Int. Ed.* **2016**, *55*, 1694-1698.
[29] P. Pyykko, *Chem. Soc. Rev.* **2008**, *37*, 1967-1997.
[30] S. Rizzato, J. Bergès, S. A. Mason, A. Albinati, J. Kozelka, *Angew. Chem. Int. Ed.* **2010**, *49*, 7440-7443.
[31] J. Kozelka. In Noncovalent Forces; Scheiner, S., Ed.; Springer: Dordrecht, 2015, p 129-158.
[32] E. S. Kryachko, *J. Mol. Struct.* **2008**, *880*, 23-30.
[33] I. Alkorta, J. Elguero, S. J. Grabowski, *Phys. Chem. Chem. Phys.* **2015**, *17*, 3261-3272.
[34] S. J. Grabowski, *Phys. Chem. Chem. Phys.* **2014**, *16*, 1824-1834.

[35] W. Zierkiewicz, D. C. Bieńko, D. Michalska, T. Zeegers-Huyskens, *J. Comput. Chem.* **2015**, *36*, 821-832.
[36] P. Deepa, B. V. Pandiyan, P. Kolandaivel, P. Hobza, *Phys. Chem. Chem. Phys.* **2014**, *16*, 2038-2047.
[37] U. Adhikari, S. Scheiner, *J. Phys. Chem. A* **2012**, *116*, 3487-3497.
[38] J. P. Anable, D. E. Hird, S. L. Stephens, D. P. Zaleski, N. R. Walker, A. C. Legon, *Chem. Phys. Lett.* **2015**, *625*, 179-185.
[39] P. Politzer, J. S. Murray. In Noncovalent Forces; Scheiner, S., Ed.; Springer: Dordrecht, Netherlands, 2015, p 357-389.
[40] S. Scheiner, *CrystEngComm* **2013**, *15*, 3119-3124.
[41] U. Adhikari, S. Scheiner, *Chem. Phys. Lett.* **2012**, *532*, 31-35.
[42] S. Scheiner, *J. Chem. Phys.* **2011**, *134*, 164313.
[43] M. Iwaoka, S. Takemoto, S. Tomoda, *J. Am. Chem. Soc.* **2002**, *124*, 10613-10620.
[44] V. d. P. N. Nziko, S. Scheiner, *J. Org. Chem.* **2015**, *80*, 2356-2363.
[45] V. d. P. N. Nziko, S. Scheiner, *J. Phys. Chem. A* **2014**, *118*, 10849-10856.
[46] L. M. Azofra, S. Scheiner, *J. Phys. Chem. A* **2014**, *118*, 3835-3845.
[47] K. W. Klinkhammer, P. Pyykko, *Inorg. Chem.* **1995**, *34*, 4134-4138.
[48] S. Scheiner, *J. Chem. Phys.* **2011**, *134*, 094315.
[49] A. Bauzá, T. J. Mooibroek, A. Frontera, *ChemPhysChem.* **2015**, *16*, 2496-2517.
[50] J. E. Del Bene, I. Alkorta, J. Elguero. In Noncovalent Forces; Scheiner, S., Ed.; Springer: Dordrecht, Netherlands, 2015, p 191-263.
[51] S. Scheiner, *Acc. Chem. Res.* **2013**, *46*, 280-288.
[52] D. Hadzi, S. Bratos. In The Hydrogen Bond. Recent Developments in Theory and Experiments; Schuster, P.; Zundel, G.; Sandorfy, C., Eds.; North-Holland Publishing Co.: Amsterdam, 1976, p 565-611.
[53] P. Schuster. Hydrogen Bonds; Springer-Verlag: Berlin, 1984.
[54] P. Schuster, G. Zundel, C. Sandorfy, Eds. The Hydrogen Bond. Recent Developments in Theory and Experiments; North-Holland Publishing Co.: Amsterdam, 1976.
[55] Z. S. Derewenda, L. Lee, U. Derewenda, *J. Mol. Biol.* **1995**, *252*, 248-262.
[56] S. Horowitz, R. C. Trievel, *J. Biol. Chem.* **2012**, *287*, 41576-41582.
[57] G. R. Desiraju, T. Steiner. The Weak Hydrogen Bond in Structural Chemistry and Biology; Oxford: New York, 1999.
[58] G. R. Desiraju, *Acc. Chem. Res.* **1996**, *29*, 441-449.
[59] M. C. Wahl, M. Sundaralingam, *Trends Biochem. Sci.* **1997**, *22*, 97-102.
[60] R. K. Castellano, *Curr. Org. Chem.* **2004**, *8*, 845-865.
[61] S. Yohannan, S. Faham, D. Yang, D. Grosfeld, A. K. Chamberlain, J. U. Bowie, *J. Am. Chem. Soc.* **2004**, *126*, 2284 - 2285.
[62] M. Mottamal, T. Lazaridis, *Biochem.* **2005**, *44*, 1607-1613.
[63] C. R. Jones, P. K. Baruah, A. L. Thompson, S. Scheiner, M. D. Smith, *J. Am. Chem. Soc.* **2012**, *134*, 12064-12071.
[64] P. Seiler, J. D. Dunitz, *Helv. Chim. Acta* **1989**, *72*, 1125-1135.
[65] M. J. Frisch, G. W. Trucks, H. B. Schlegel, G. E. Scuseria, M. A. Robb, J. R. Cheeseman, G. Scalmani, V. Barone, B. Mennucci, G. A. Petersson, H. Nakatsuji, M. Caricato, X. Li, H. P. Hratchian, A. F. Izmaylov, J. Bloino, G. Zheng, J. L. Sonnenberg, M. Hada, M. Ehara, K. Toyota, R. Fukuda, J. Hasegawa, M. Ishida, T. Nakajima, Y. Honda, O. Kitao, H. Nakai, T. Vreven, J. Montgomery, J. A., J. E. Peralta, F. Ogliaro, M. Bearpark, J. J. Heyd, E. Brothers, K. N. Kudin, V. N. Staroverov, R. Kobayashi, J. Normand, K. Raghavachari, A. Rendell, J. C. Burant, S. S. Iyengar, J. Tomasi, M. Cossi, N. Rega, J. M. Millam, M. Klene, J. E. Knox, J. B. Cross, V. Bakken, C. Adamo, J. Jaramillo, R. Gomperts, R. E. Stratmann, O. Yazyev, A. J. Austin, R. Cammi, C. Pomelli, J. W. Ochterski, R. L. Martin, K. Morokuma, V. G. Zakrzewski, G. A. Voth, P. Salvador,

J. J. Dannenberg, S. Dapprich, A. D. Daniels, O. Farkas, J. B. Foresman, J. V. Ortiz, J. Cioslowski, D. J. Fox. Wallingford, CT, 2009.
[66] H.-J. Werner, P. J. Knowles, F. R. Manby, M. Schütz, P. Celani, G. Knizia, T. Korona, R. Lindh, A. Mitrushenkov, G. Rauhut, T. B. Adler, R. D. Amos, A. Bernhardsson, A. Berning, D. L. Cooper, M. J. O. Deegan, A. J. Dobbyn, F. Eckert, E. Goll, C. Hampel, A. Hesselmann, G. Hetzer, T. Hrenar, G. Jansen, C. Köppl, Y. Liu, A. W. Lloyd, R. A. Mata, A. J. May, S. J. McNicholas, W. Meyer, M. E. Mura, A. Nicklaß, P. Palmieri, K. Pflüger, R. Pitzer, M. Reiher, T. Shiozaki, H. Stoll, A. J. Stone, R. Tarroni, T. Thorsteinsson, M. Wang, A. Wolf. 2010.
[67] B. L. Bedell, L. Goldfarb, E. R. Mysak, C. Samet, A. Maynard, *J. Phys. Chem. A* **1999**, *103*, 4572-4579.
[68] N. Karger, A. M. Amorim da Costa, J. A. Ribeiro-Claro, *J. Phys. Chem. A* **1999**, *103*, 8672-8677.
[69] P. Hobza, Z. Havlas, *Chem. Rev.* **2000**, *100*, 4253-4264.
[70] M. P. M. Marques, A. M. A. da Costa, P. J. A. Ribeiro-Claro, *J. Phys. Chem. A* **2001**, *105*, 5292-5297.
[71] R. Gopi, N. Ramanathan, K. Sundararajan, *J. Phys. Chem. A* **2014**, *118*, 5529-5539.
[72] Y. Gu, T. Kar, S. Scheiner, *J. Am. Chem. Soc.* **1999**, *121*, 9411-9422.
[73] M. Nishio, Y. Umezawa, J. Fantini, M. S. Weiss, P. Chakrabarti, *Phys. Chem. Chem. Phys.* **2014**, *16*, 12648-12683.
[74] H. K. Ganguly, B. Majumder, S. Chattopadhyay, P. Chakrabarti, G. Basu, *J. Am. Chem. Soc.* **2012**, *134*, 4661-4669.
[75] O. Takahashi, Y. Kohno, M. Nishio, *Chem. Rev.* **2010**, *110*, 6049-6076.
[76] S. Scheiner, T. Kar, J. Pattanayak, *J. Am. Chem. Soc.* **2002**, *124*, 13257-13264.
[77] E. Steiner, P. W. Fowler, L. W. Jenneskens, *Angew. Chem. Int. Ed.* **2001**, *40*, 362-366.
[78] P. v. R. Schleyer, C. Maerker, A. Dransfeld, H. Jiao, N. J. R. v. E. Hommes, *J. Am. Chem. Soc.* **1996**, *118*, 6317-6318.
[79] E. Kleinpeter, S. Klod, A. Koch, *J. Mol. Struct. Theochem* **2007**, *811*, 45-60.
[80] E. Kleinpeter, A. Koch, *Phys. Chem. Chem. Phys.* **2012**, *14*, 8742-8746.
[81] K. E. Horner, P. B. Karadakov, *J. Org. Chem.* **2015**, *80*, 7150-7157.
[82] P. B. Karadakov, K. E. Horner, *J. Chem. Theory Comput.* **2016**, *12*, 558-563.
[83] I. Alkorta, J. Elguero, *New J. Chem.* **1998**, *22*, 381-385.
[84] A. Masunov, J. J. Dannenberg, R. H. Contreras, *J. Phys. Chem. A* **2001**, *105*, 4737-4740.
[85] L. Pejov, K. Hermansson, *J. Chem. Phys.* **2003**, *119*, 313-324.
[86] W. Qian, S. Krimm, *J. Phys. Chem. A* **2002**, *106*, 11663-11671.
[87] X. Li, L. Liu, H. B. Schlegel, *J. Am. Chem. Soc.* **2002**, *124*, 9639-9647.
[88] I. V. Alabugin, M. Manoharan, F. A. Weinhold, *J. Phys. Chem. A* **2004**, *108*, 4720 - 4730.
[89] J. Joseph, E. D. Jemmis, *J. Am. Chem. Soc.* **2007**, *129*, 4620-4632.
[90] B. Michielsen, W. A. Herrebout, B. J. van der Veken, *ChemPhysChem.* **2008**, *9*, 1693-1701.
[91] A. Karpfen, *Phys. Chem. Chem. Phys.* **2011**, *13*, 14194-14201.
[92] Y. Mo, C. Wang, L. Guan, B. Braïda, P. C. Hiberty, W. Wu, *Chem. Eur. J.* **2014**, *20*, 8444–8452.
[93] M. Jabłoński, *J. Comput. Chem.* **2014**, *35*, 1739-1747.
[94] M. D. Struble, C. Kelly, M. A. Siegler, T. Lectka, *Angew. Chem. Int. Ed.* **2014**, *53*, 8924-8928.
[95] M. Saggu, N. M. Levinson, S. G. Boxer, *J. Am. Chem. Soc.* **2012**, *134*, 18986-18997.
[96] W. Qian, S. Krimm, *J. Phys. Chem. A* **2002**, *106*, 6628-6636.
[97] K. Hermansson, *J. Phys. Chem. A* **2002**, *106*, 4695-4702.
[98] S. N. Delanoye, W. A. Herrebout, B. J. van der Veken, *J. Am. Chem. Soc.* **2002**, *124*, 7490-7498.

Table 1. Interaction energy, change in chemical shielding of bridging proton, and O-H stretching frequency in water dimer as two water molecules are pushed together

ΔR(H··O), Å	E_{int}, kcal/mol	$\Delta\sigma^{a}$, ppm	$\Delta\nu^{a,b}$, cm^{-1}	E_{att}^{c}, kcal/mol
0	-5.18	-2.96	-104.9	-14.1
-0.2	-4.53	-4.48	-130.1	-22.9
-0.4	-1.38	-6.98	-174.3	-39.3
-0.6	+7.63	-10.97	-229.7	-71.0
-0.8	+29.93	-16.83	-169.5	-133.1

[a]relative to isolated monomer

[b]asymmetric stretch that most heavily involves bridging proton

[c]total attractive forces: electrostatic + induction + dispersion

Table 2. Interaction energy, changes in chemical shielding of bridging proton and C-H stretching frequency in $H_3CH\cdots OH_2$ as two molecules are pushed together

ΔR(H··O), Å	E_{int}, kcal/mol	Δσ, ppm	$\Delta\nu^{a}$, cm^{-1}	E_{att}^{b}, kcal/mol
0	-0.74	-1.02	1.5	-2.0
-0.2	-0.64	-1.33	5.3	-3.2
-0.4	-0.14	-1.84	10.8	-5.5
-0.6	+1.19	-2.72	18.3	-9.9
-0.8	+4.22	-4.25	27.8	-18.4

[a]asymmetric stretch that most heavily involves bridging proton

[b]total attractive forces: electrostatic + induction + dispersion

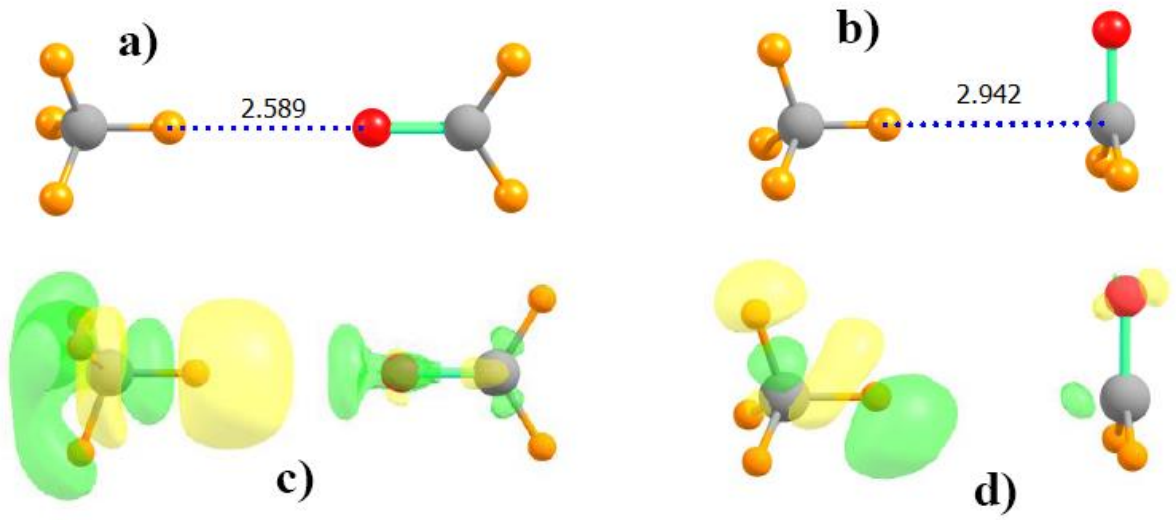

Fig 1. Geometries of $H_3CH\cdot\cdot OCH_2$, wherein a) the bridging proton lies directly along the C··O axis and b) the C-H bond lies directly above the C of OCH_2, and is perpendicular to the molecular plane. Electron density shifts in c and d are illustrated at the ±0.0002 au contour wherein density gains are indicated in green and losses in yellow.

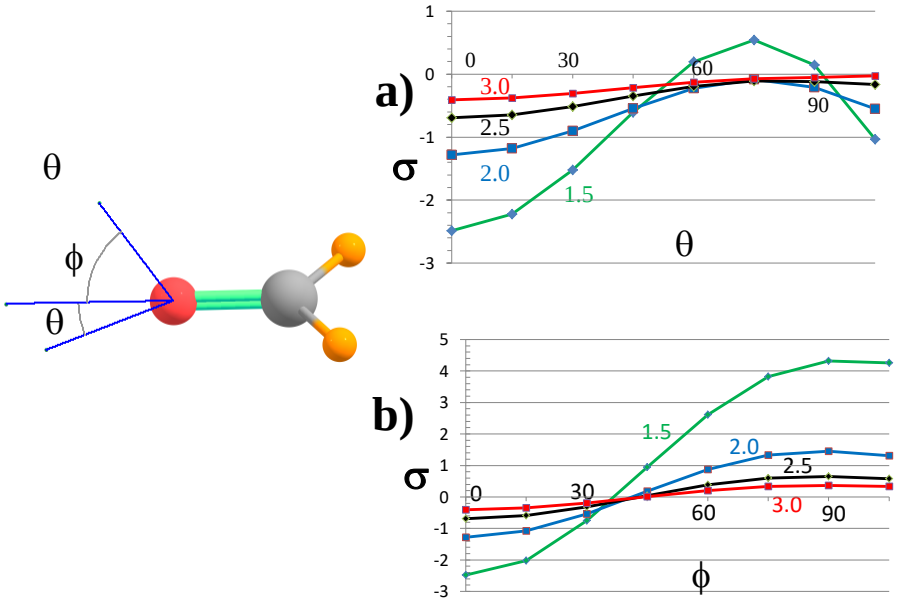

Fig 2. NMR chemical shielding σ (ppm) at various locations around H_2CO. Each curve is labeled by R (Å), the distance from the O atom. a) θ and b) φ refer respectively to in-plane and out-of-plane deviations (degs) from the C=O axis.

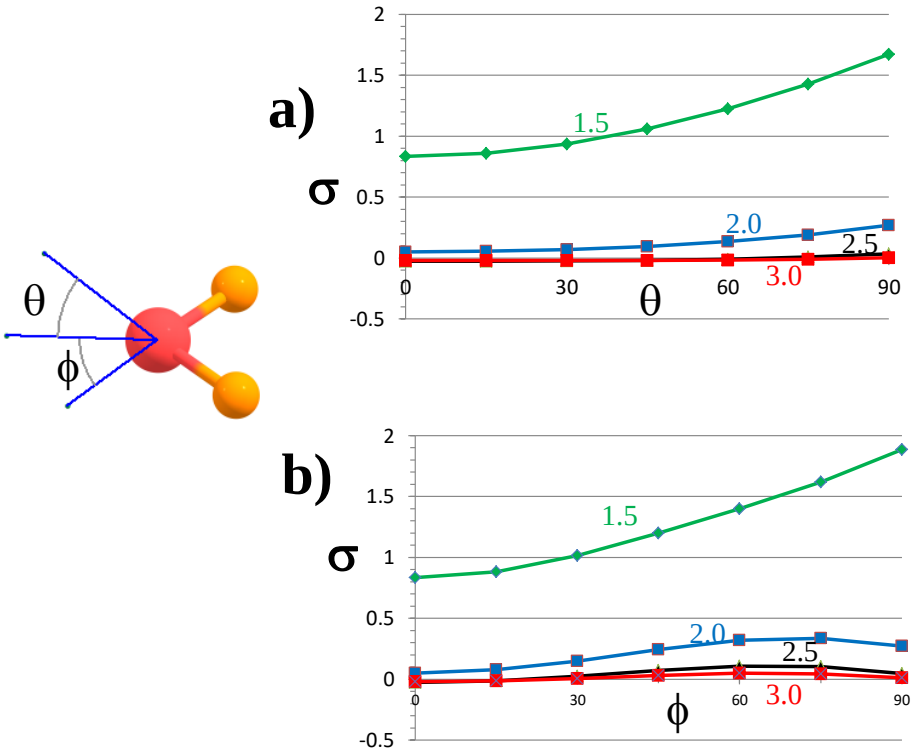

Fig 3. NMR chemical shielding σ (ppm) at various locations around H_2O. Each curve is labeled by R (Å), the distance from the O atom. a) θ and b) φ refer respectively to in-plane and out-of-plane deviations (degs) from the plane containing the two rabbit-ear O lone pairs, perpendicular to the HOH molecular plane.

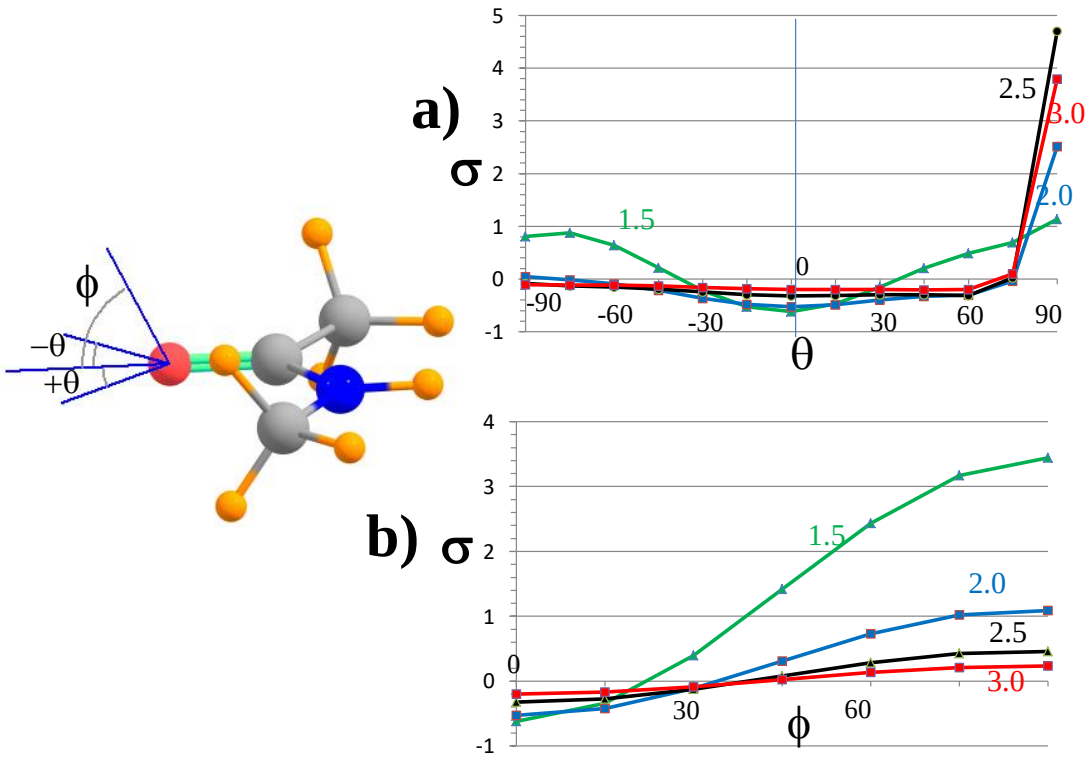

Fig 4. NMR chemical shielding σ (ppm) at various locations around N-methylacetamide. Each curve is labeled by R (Å), the distance from the O atom. a) θ and b) φ refer respectively to in-plane and out-of-plane deviations (degs) from the CCONC molecular plane.

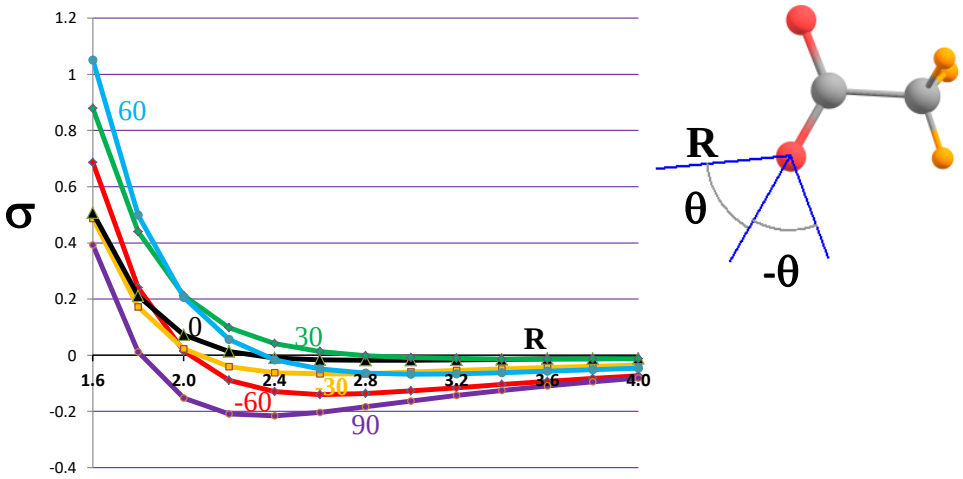

Fig 5. NMR chemical shielding σ (ppm) at various locations around CH_3COO^-. Each curve is labeled by the deviation from the indicated C-O axis θ (degs) within the OOCC molecular plane, and is shown as a function of R, the distance (Å) of the reference point from the O atom.

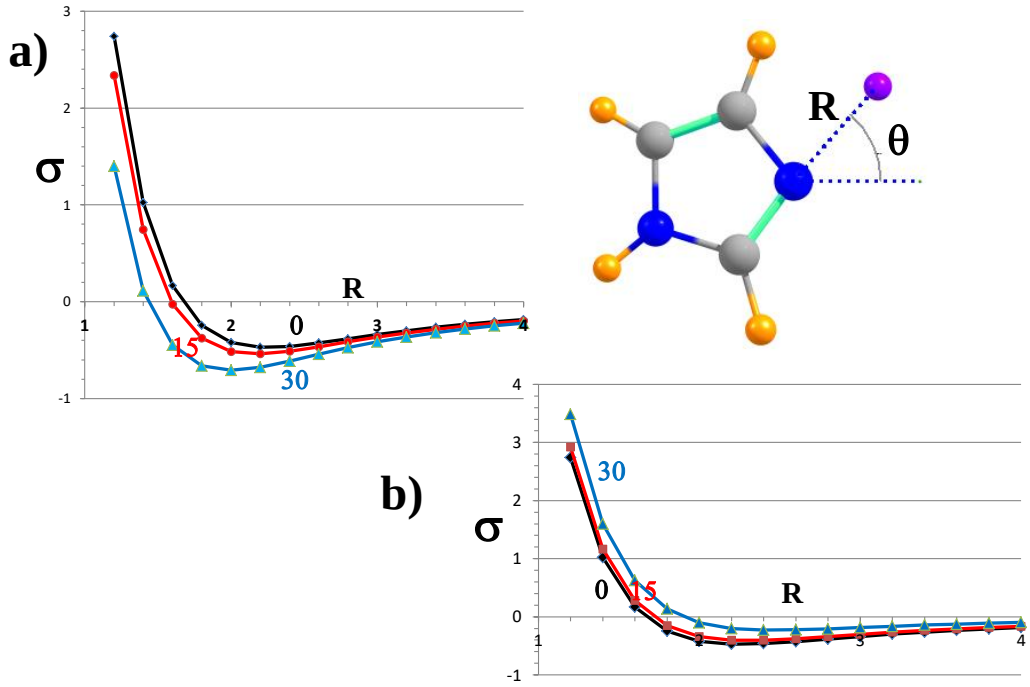

Fig 6. NMR chemical shielding σ (ppm) at various locations around the indicated N atom of imidazole. Each curve is labeled by the deviation from the indicated C-O axis both in the molecular plane a) θ (degs) and out of this plane b) φ. R refers to the distance (Å) of the reference point from the N atom.

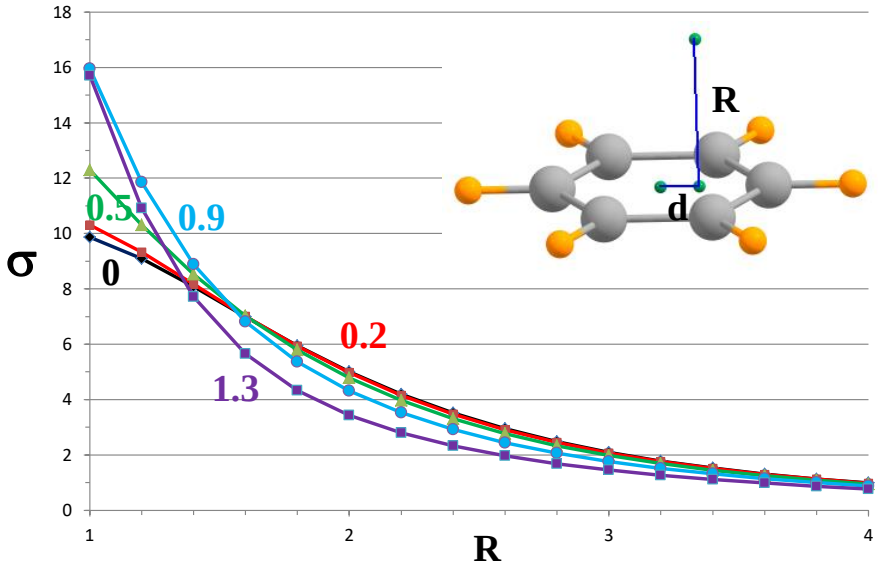

Fig 7. NMR chemical shielding σ (ppm) at various locations around the benzene molecule. Each curve is labeled by the displacement d (Å) of the point of reference from the benzene center.

NMR chemical shielding can be caused simply by proximity to H-bond acceptor, in absence of proton donor